Supplementary Information

Synergic antimony-niobium pentoxide nanomeshes for high-rate sodium storage

Liu Wang, and Xiaofang Bi, Shubin Yang**

Fabrication of the synergic Sb-Nb_2O_5 nanomeshes

$Nb_2O_5\cdot nH_2O$ nanosheets were firstly synthesized via a hydrothermal treatment using $NbCl_5$ as precursor. Typically, 5 mmol $NbCl_5$ was added into 50 mL $NH_3\cdot H_2O$ aqueous solution (pH 8), forming a translucent white dispersion. After magnetic stirring for 2 h, a hydrothermal treatment at 240 ºC was carried out for 24 h. The $Nb_2O_5\cdot nH_2O$ nanosheets were obtained by washing with deionized water, centrifuging and freeze-drying. Then 20 mg $Nb_2O_5\cdot nH_2O$ nanosheets were suspended in 50 mL ethanol containing 50 uL $NH_3\cdot H_2O$ (28 wt.%) and 0.2 g cetyltrimethyl ammonium bromide (CTAB). After ultrasonically treating for 0.5 h, 60 mg $SbCl_3$ dissolved in 0.2 mL ethanol was added dropwise into the abovementioned dispersion under magnetic stirring. During this process, antimony source was deposited on the surfaces of CTAB modified $Nb_2O_5\cdot nH_2O$ nanosheets. An annealing treatment was subsequently carried out at 550 ºC under Ar atmosphere, generating $SbNbO_4$ nanosheets, which maintain the morphology of the $Nb_2O_5\cdot nH_2O$ nanosheets. Finally, the resulting $SbNbO_4$ nanosheets were calcinated under reducing atmosphere of H_2/Ar (10 vol% of H_2) at 600 ºC for various time from 10 min to 3 h. A typical annealing time is 3 h, thus the synergic Sb-Nb_2O_5 nanomeshes were obtained.

Structural characterizations

The morphology, microstructure and crystal structure of the samples were investigated by SEM (Zeiss Supera 55), TEM (JEOL 2100F), XRD (Rigaku D/MAX2200pc) measurements. The compositions of the samples were inspected by XPS (Thermo Escalab 250XI), Raman

(Renishaw Invia) and TG (NETZSCH STA 449 F3 Jupiter). The nitrogen physisorption measurements were performed on a Quantachrome QDS-MP-30 analyzer (USA) at 77 K.

Electrochemical measurements

Electrochemical experiments were carried out using standard CR2032 type coin cells. The working electrodes were prepared by mixing the active materials, acetylene black and Carboxy Methylated Cellulose (CMC) in deionized water, coated uniformly on pure Cu foil, and dried at 80 ºC under vacuum for 12 h. The loading mass of the active materials on the electrode is 0.4~0.6 mg cm^{-2}. Pure sodium foil was used as the counter electrode, glass fiber as the separator, and a solution of 1 M $NaClO_4$ in ethylene carbonate (EC)/ Propylene carbonate (PC) (1:1 by volume) with 5% Fluoroethylene carbonate (FEC) addition as the electrolyte. The cells were assembled in an argon-filled glove box. Galvanostatical discharge-charge experiments were tested on a Land CT2001A battery test system at different current densities in a voltage range of 0.01-2.0 V. And the specific capacity was calculated based on the mass of the entire active materials. The volumetric capacity is calculated by multiplying gravimetric capacity by electrode density based on the electrode only. In order to acquire an accurate density value, the cross-section SEM investigation was carried out on electrode with high loading mass of 1.45 mg. And the diameter of the electrode is 1.2 cm with area of 1.13 cm^2. Moreover, a pressure of 10 MPa was performed on the electrode before cross-section survey and galvanostatical discharge-charge tests for the calculation of volumetric capacity. Electrochemical impedance spectroscopy (EIS) measurements of the electrodes were carried out on an electrochemical workstation (CHI760E). The impedance spectra were obtained by applying a sine wave with amplitude of 5.0 mV over the frequency range from 100 kHz to 0.01 Hz. Fitting of impedance spectra to the proposed equivalent circuit was performed by the code Zview.

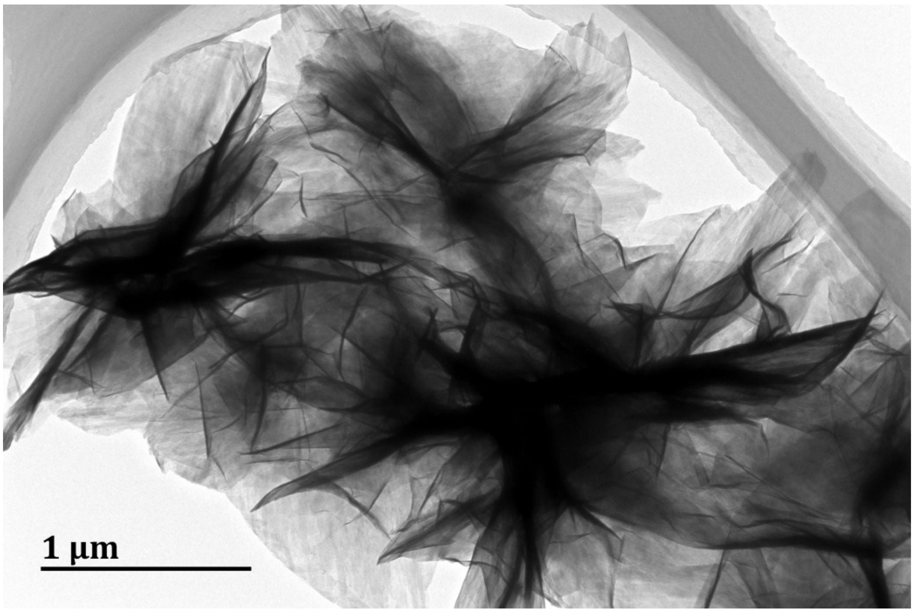

Figure S1. TEM image of $Nb_2O_5 \cdot nH_2O$ nanosheets.

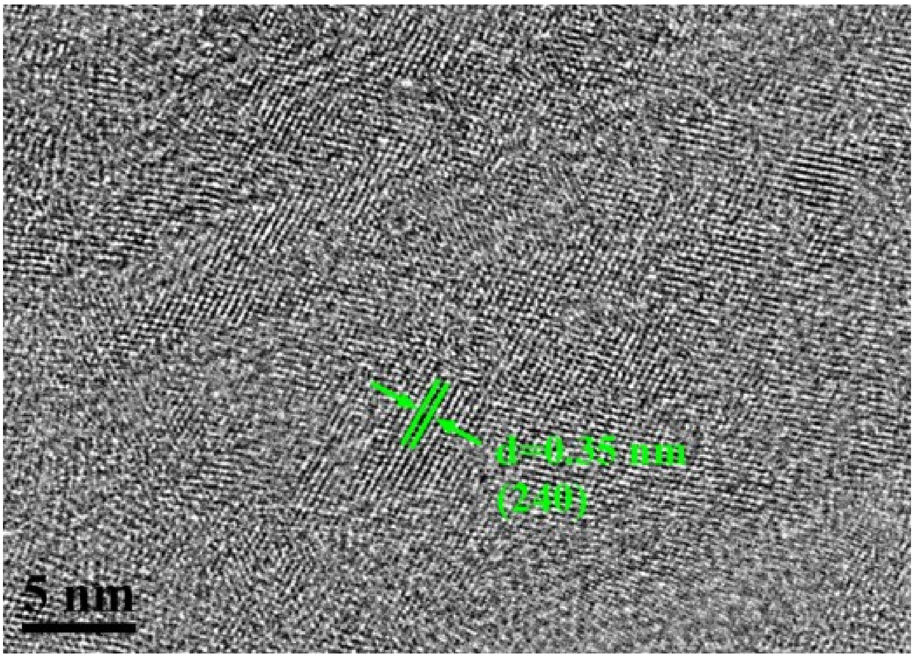

Figure S2. HRTEM image of $Nb_2O_5 \cdot nH_2O$ nanosheets.

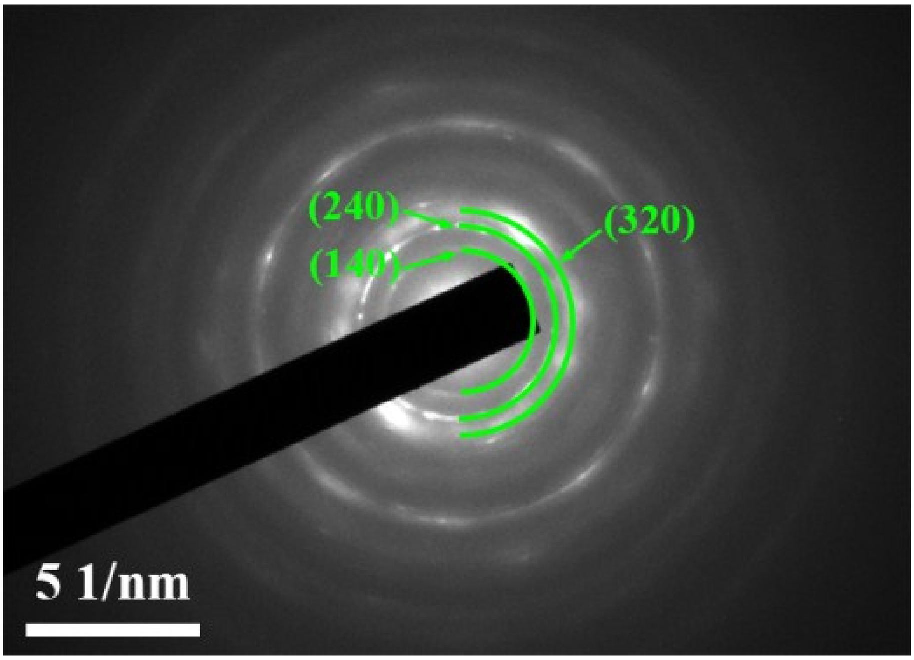

Figure S3. SEAD pattern of $Nb_2O_5 \cdot nH_2O$ nanosheets.

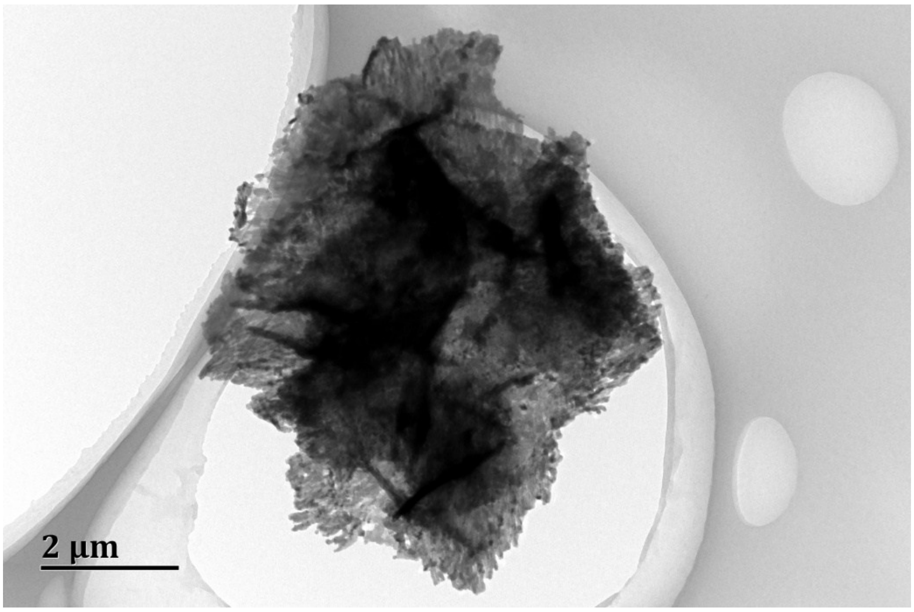

Figure S4. TEM image of $SbNbO_4$ nanosheets.

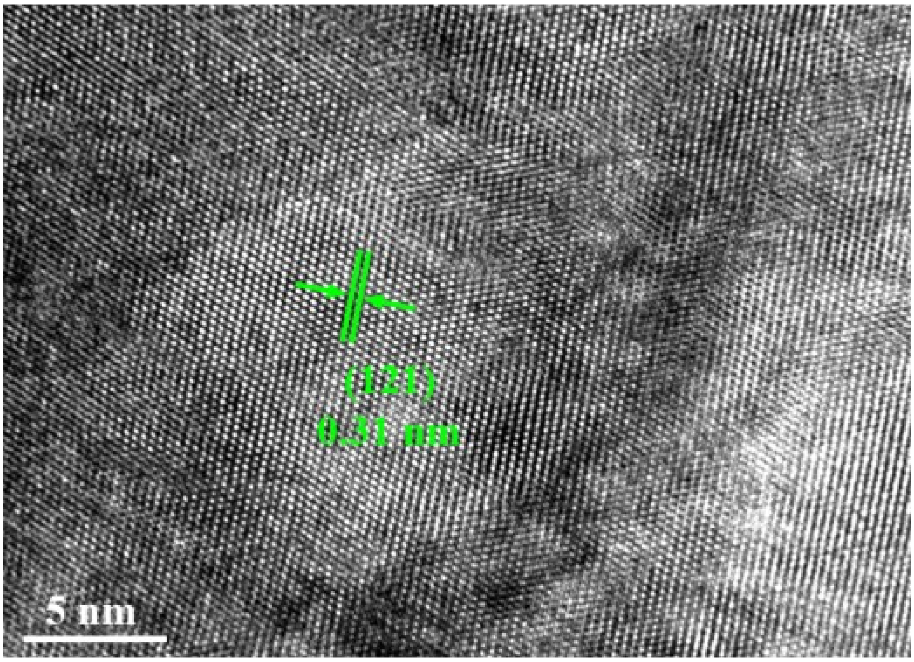

Figure S5. HRTEM image of $SbNbO_4$ nanosheets.

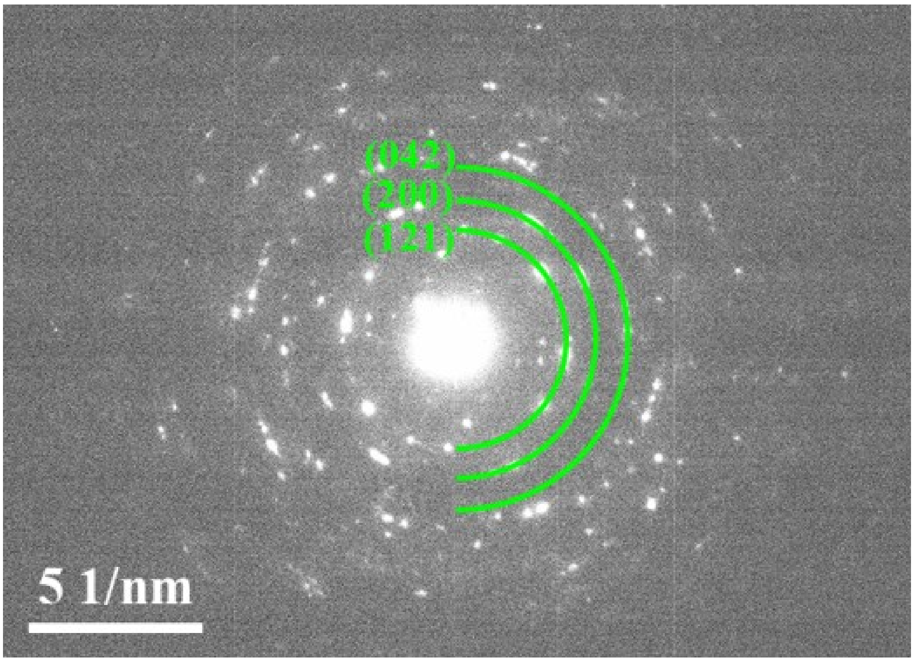

Figure S6. SEAD pattern of $SbNbO_4$ nanosheets.

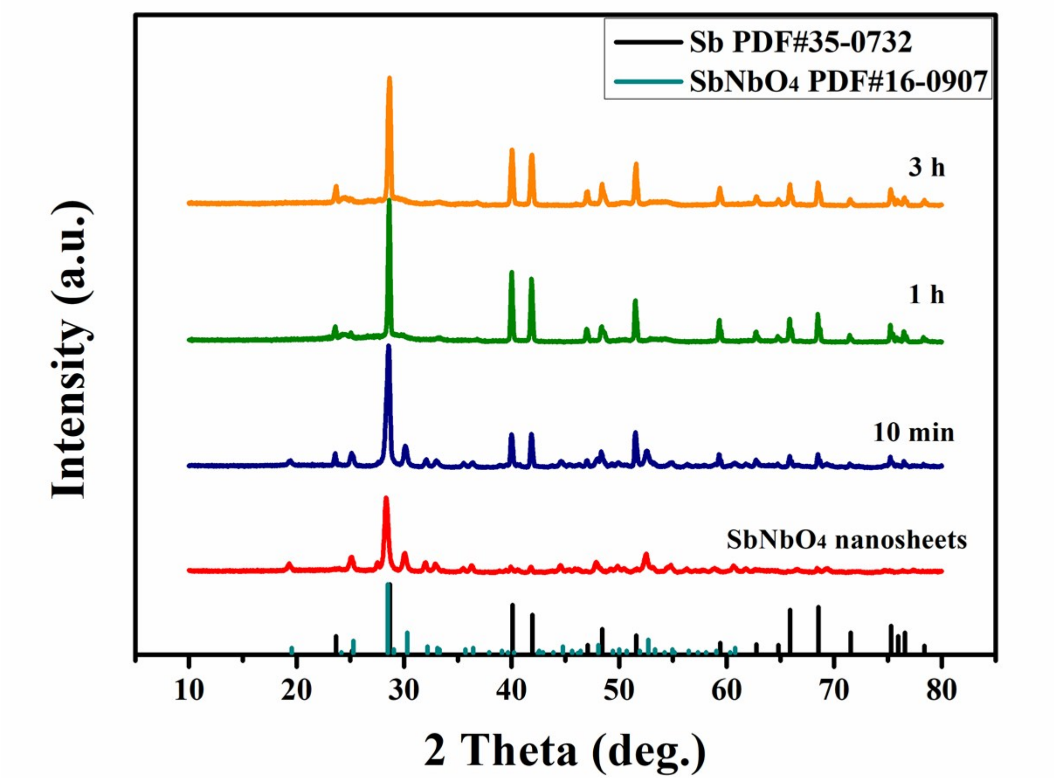

Figure S7. XRD patterns of the $SbNbO_4$ nanosheets with different decomposition time.

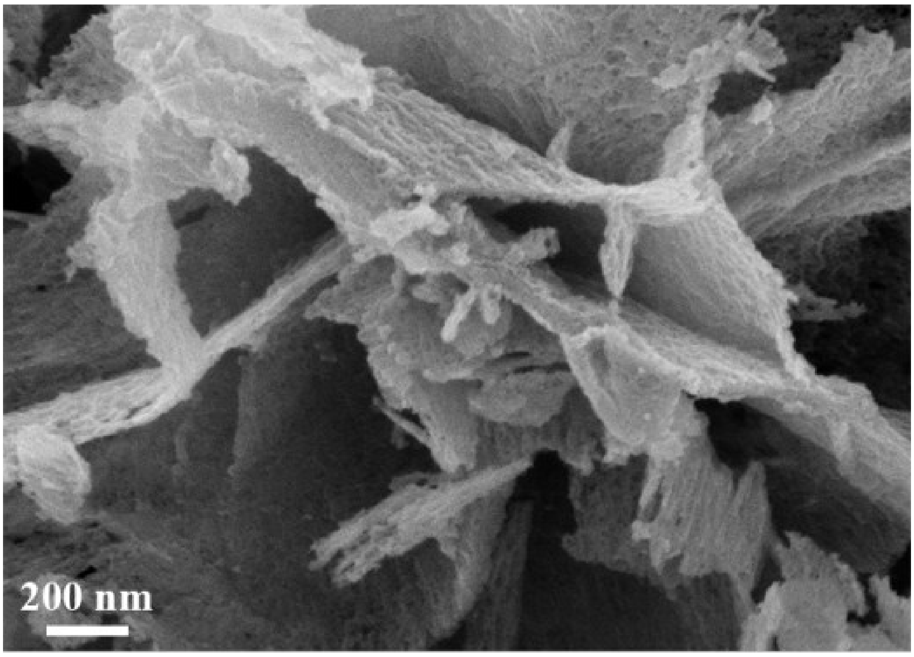

Figure S8. SEM image of 600ºC decomposition for 10 min.

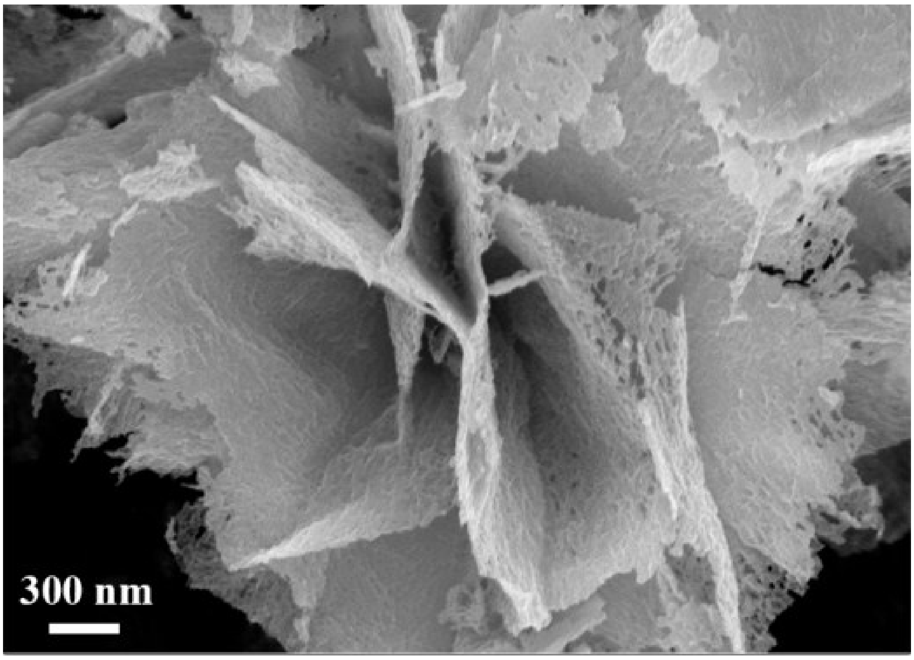

Figure S9. SEM image of 600ºC decomposition for 1 hour.

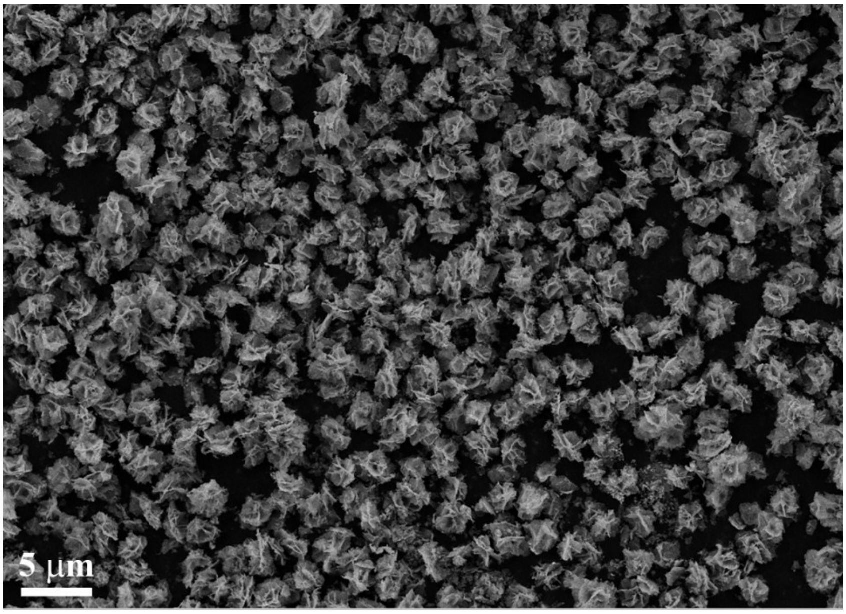

Figure S10. Low-magnified SEM image of Sb-Nb_2O_5 nanomeshes with magnification of 2,000.

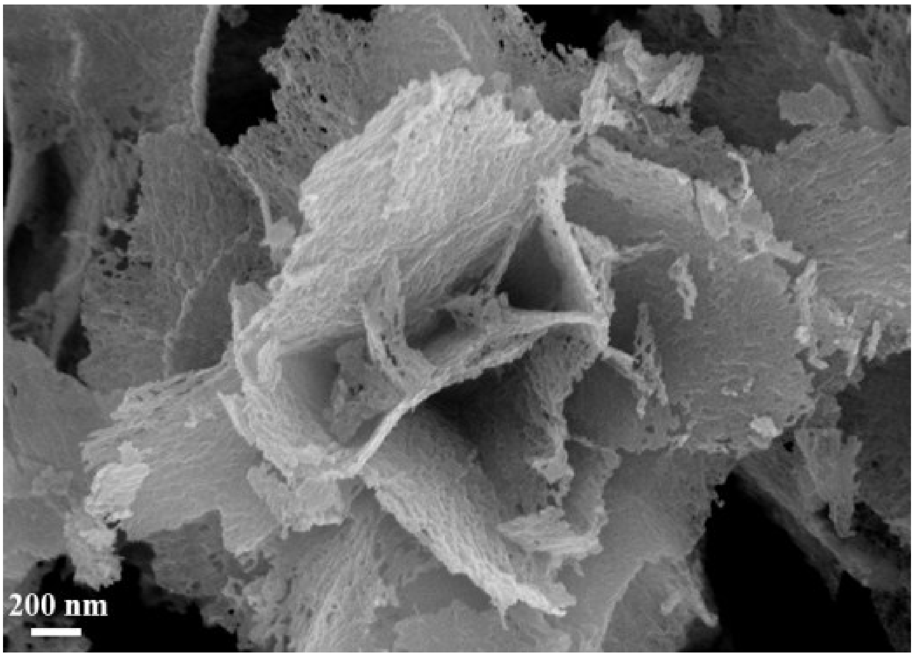

Figure S11. Magnified SEM image of Sb-Nb_2O_5 nanomeshes.

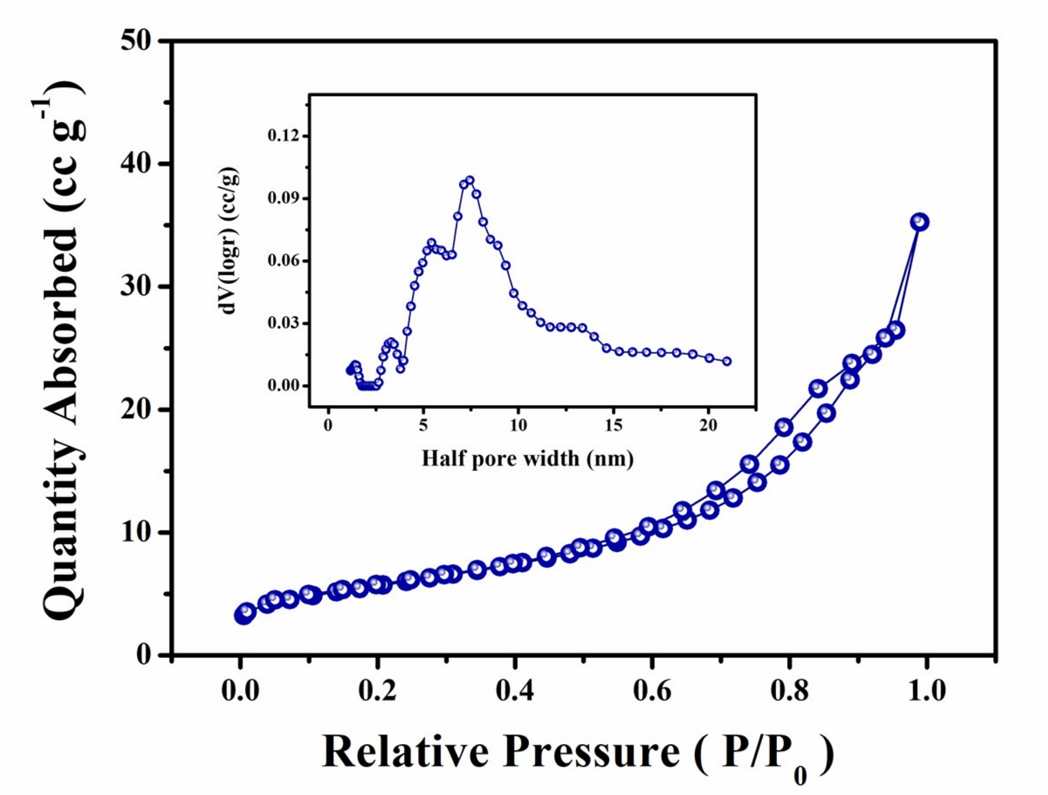

Figure S12. Nitrogen adsorption/desorption isotherms and pore size distribution (inset) of the synergic Sb-Nb_2O_5 nanomeshes, which shows a BET specific surface area of 20.4 m^2 g^{-1}.

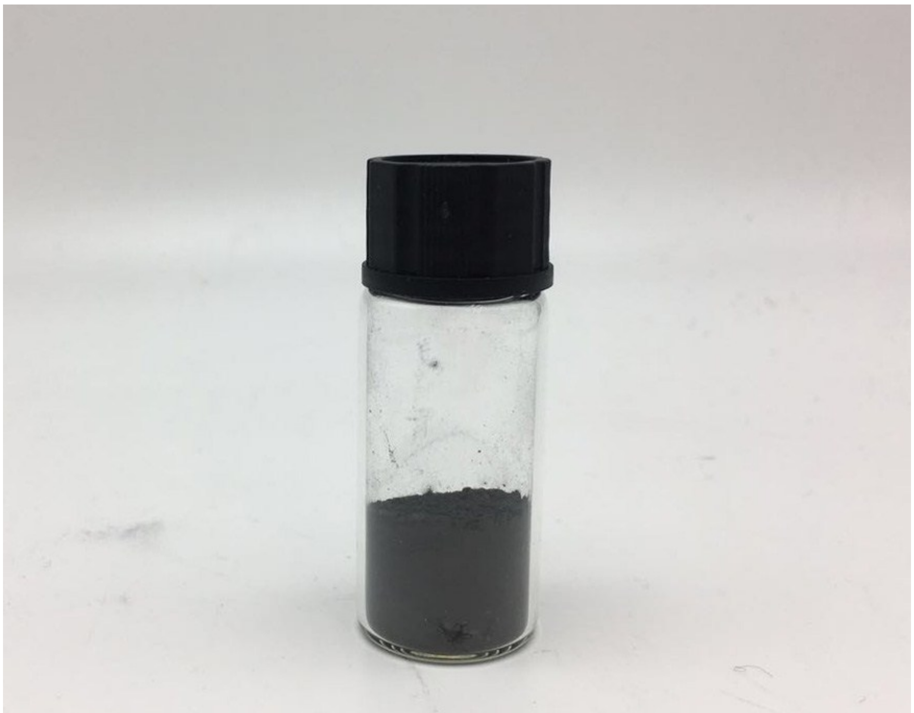

Figure S13. Optical photograph of the synergic Sb-Nb_2O_5 nanomeshes produced in large scale.

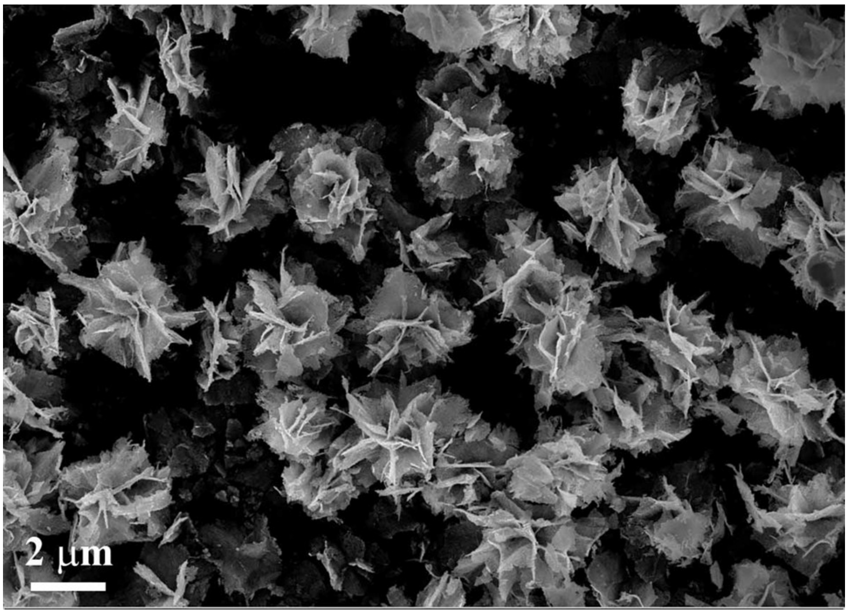

Figure S14. SEM image of the Sb-Nb_2O_5 nanomeshes produced in large scale.

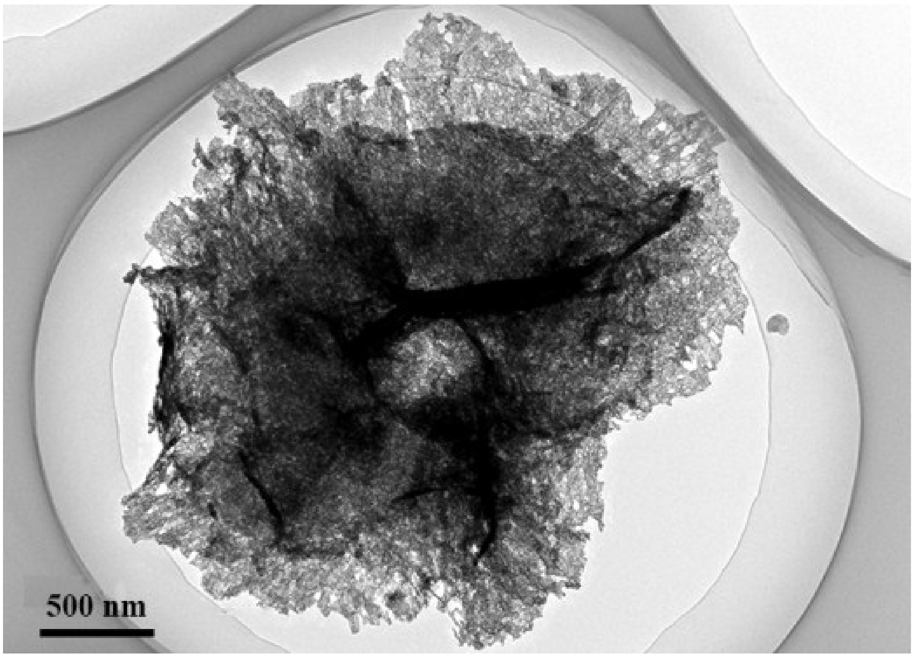

Figure S15. TEM image of the synergic Sb-Nb_2O_5 nanomeshes.

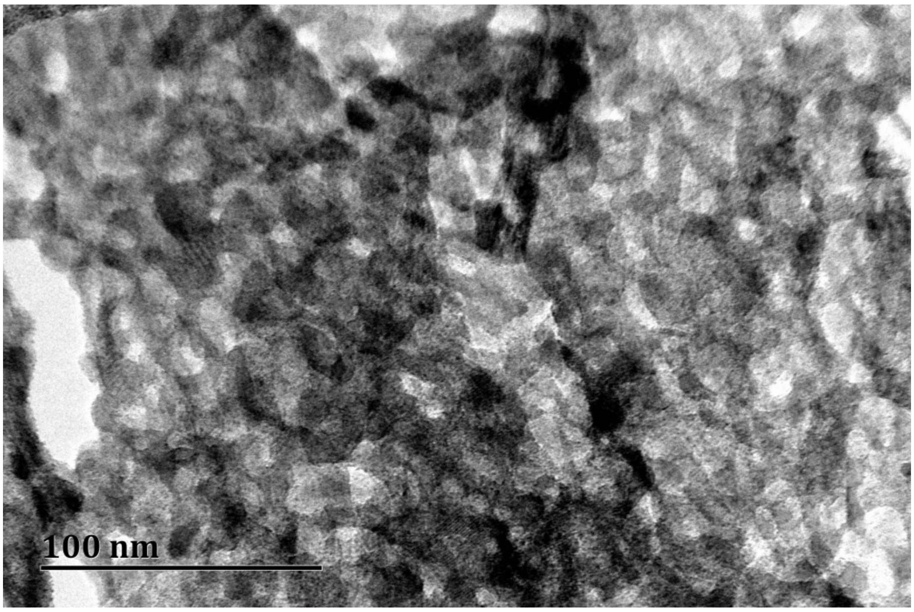

Figure S16. Magnified TEM image of the synergic Sb-Nb_2O_5 nanomeshes.

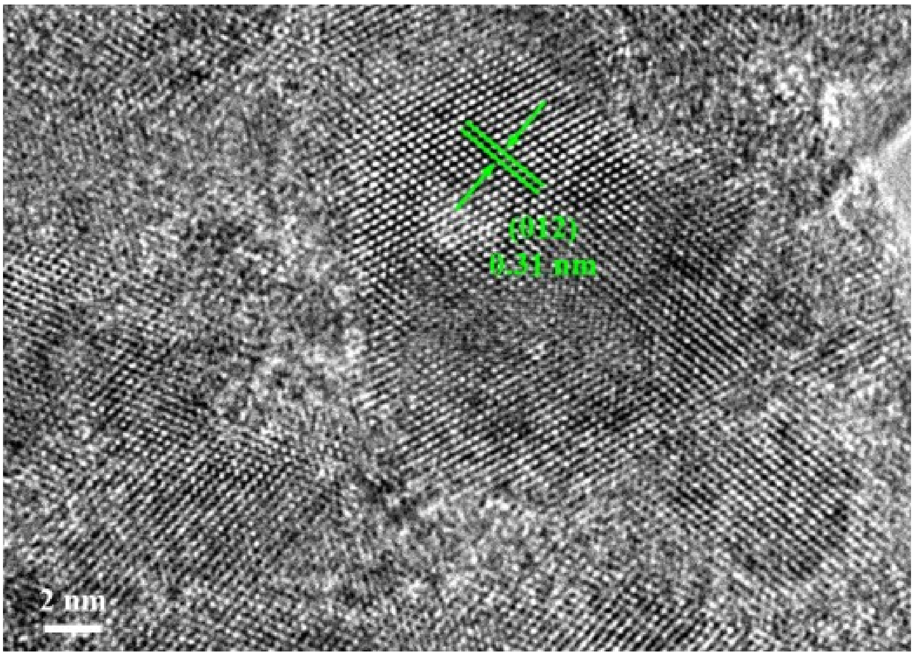

Figure S17. HRTEM image of the synergic Sb-Nb_2O_5 nanomeshes with Sb lattice fringes.

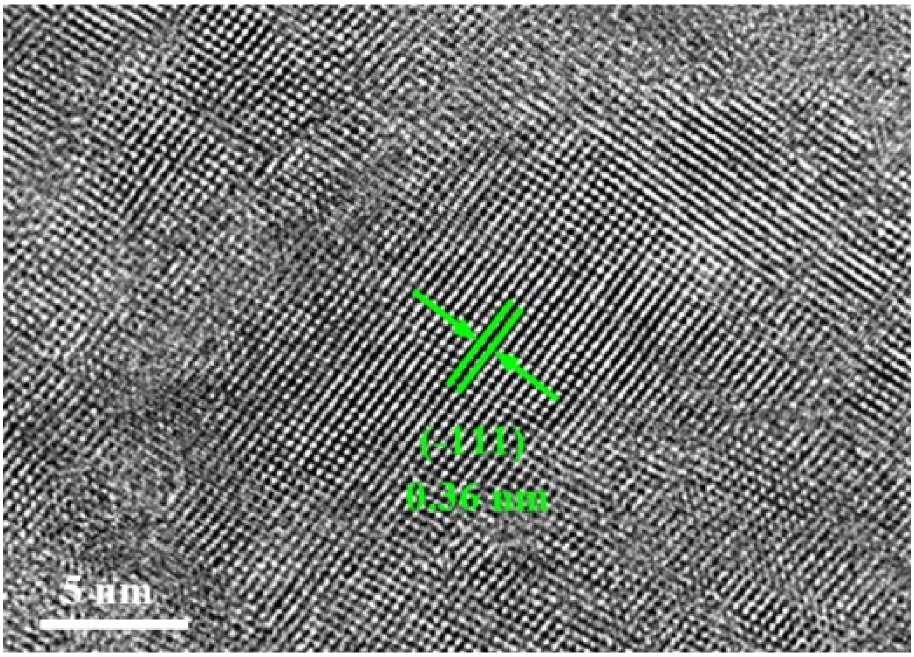

Figure S18. HRTEM image of the synergic Sb-Nb_2O_5 nanomeshes with Nb_2O_5 lattice fringes.

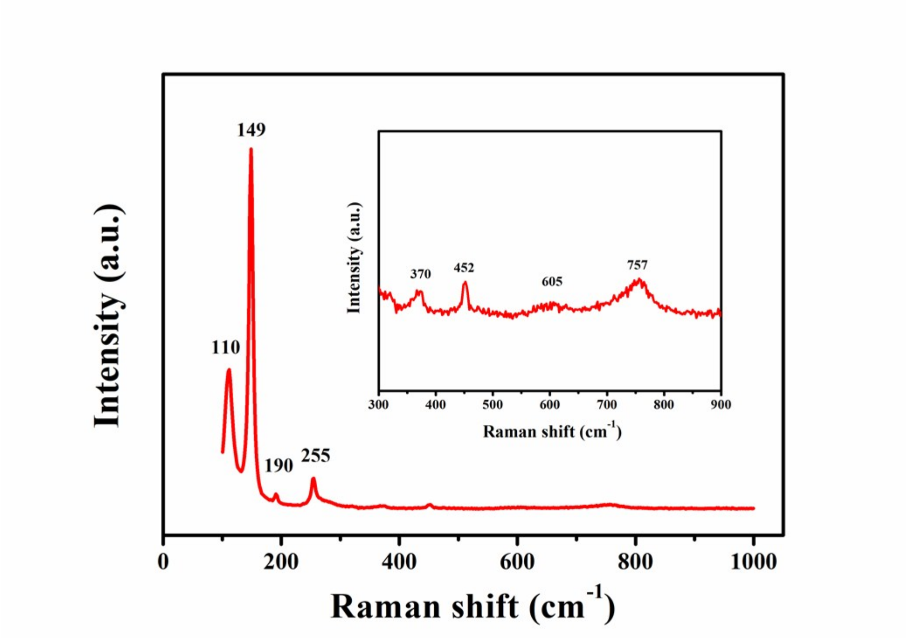

Figure S19. Raman spectrum of the synergic Sb-Nb_2O_5 nanomeshes.

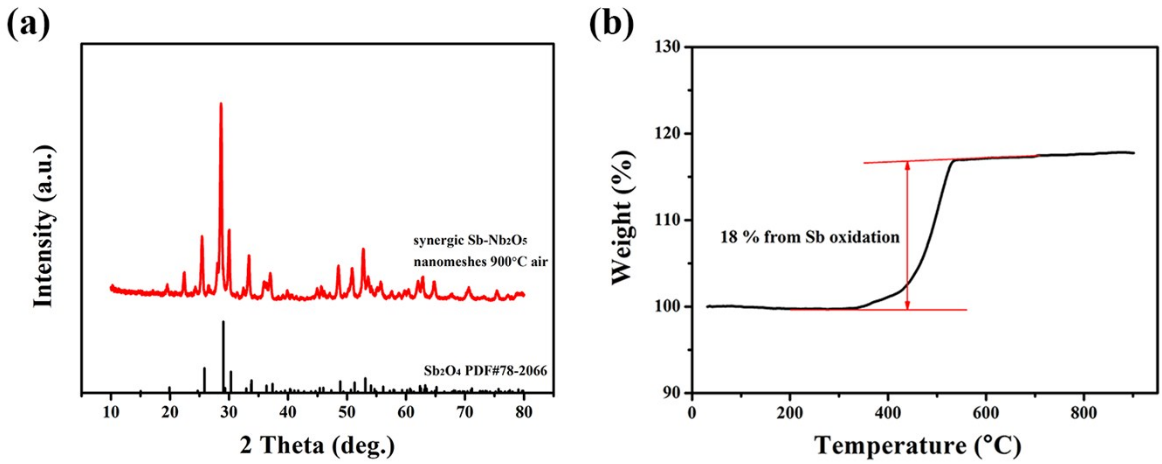

Figure S20. a) The XRD pattern demonstrates the product after Thermogravimetric (TG) measurement to be Sb_2O_4. b) TG profile of the synergic Sb-Nb_2O_5 nanomeshes. The content of Sb is calculated to be 68.6 wt.% based on the following equation: Sb (wt.%) = 100% × (2 × molecular weight of Sb) / (4 × molecular of O) × (weight increase after oxidation).

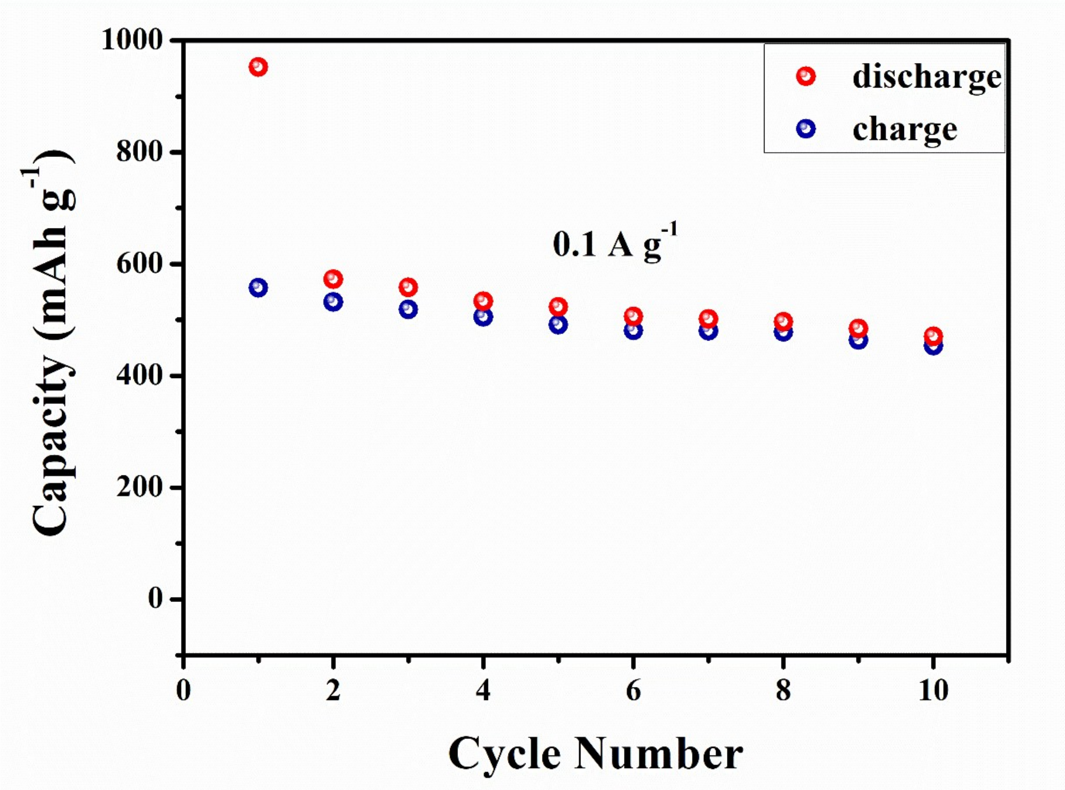

Figure S21. Discharge and charge capacities of the initial 10 cycles at 0.1 A g^{-1}.

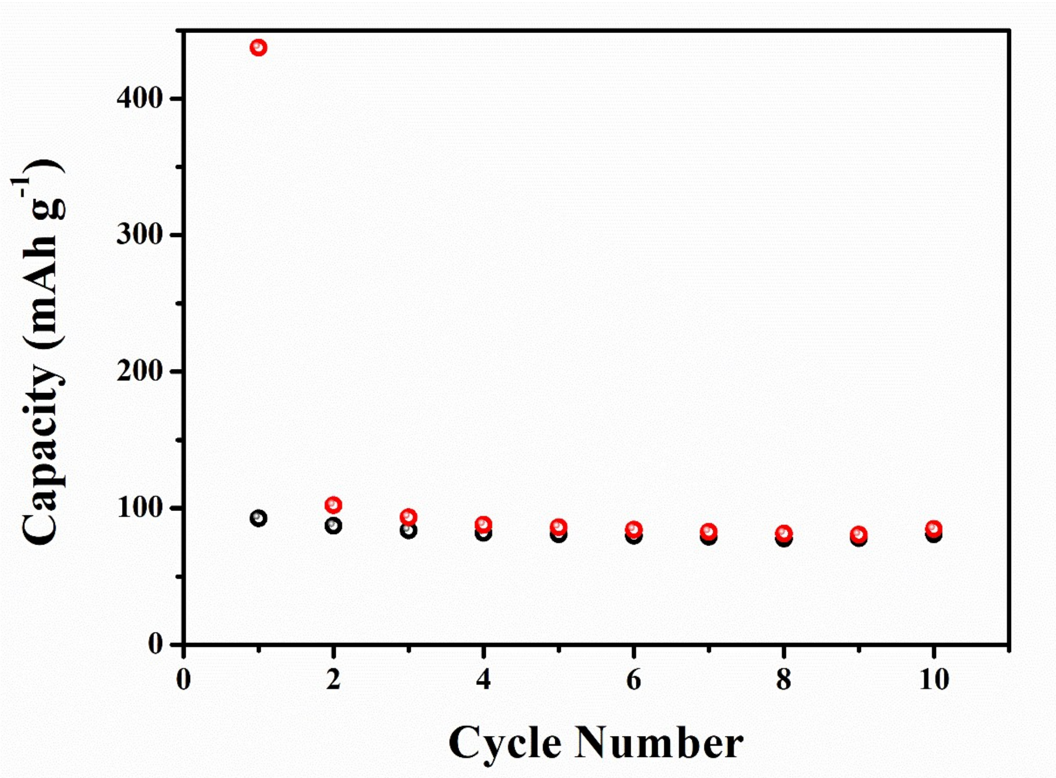

Figure S22. Discharge and charge capacities of the additive acetylene black at 0.1 A g^{-1}.

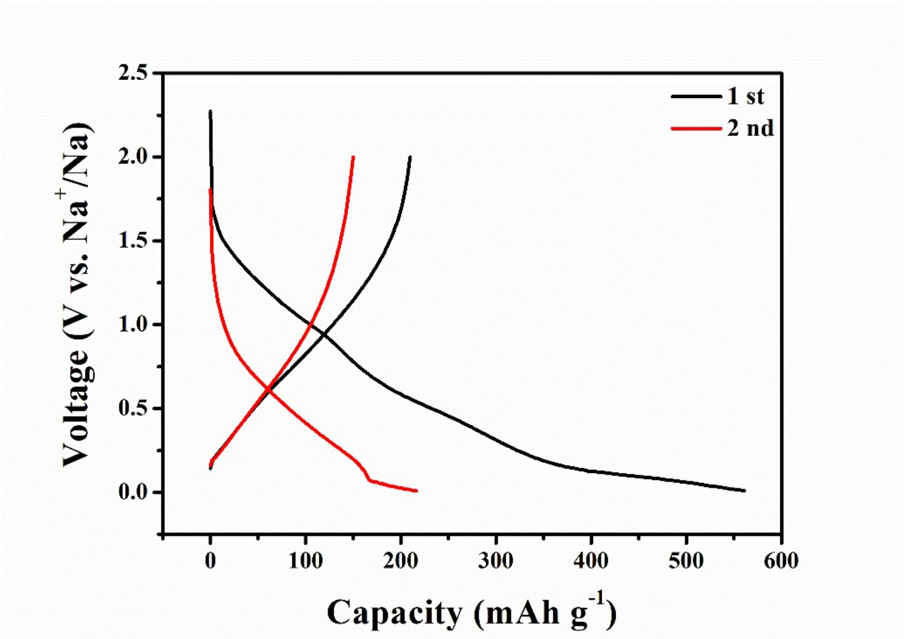

Figure S23. Charge-discharge profiles of the first two cycles at 0.1 A g^{-1} of $Nb_2O_5{\cdot}nH_2O$ nanosheets.

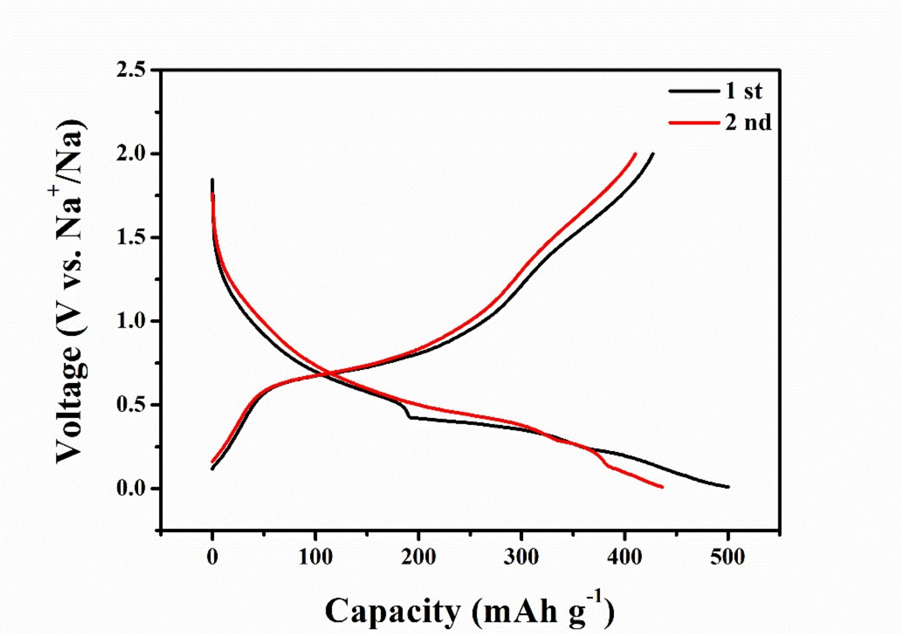

Figure S24. Charge-discharge profiles of the first two cycles at 0.1 A g^{-1} of $SbNbO_4$ nanosheets.

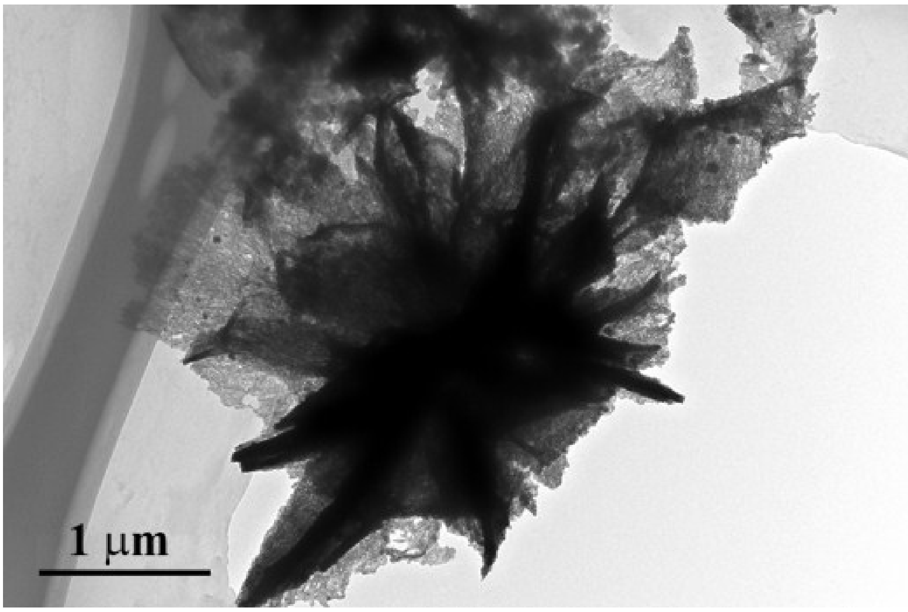

Figure S25. *Ex situ* TEM image of the synergic Sb-Nb_2O_5 nanomeshes after 100 discharge-charge cycles at 5.0 A g^{-1} with well-maintained microstructure.

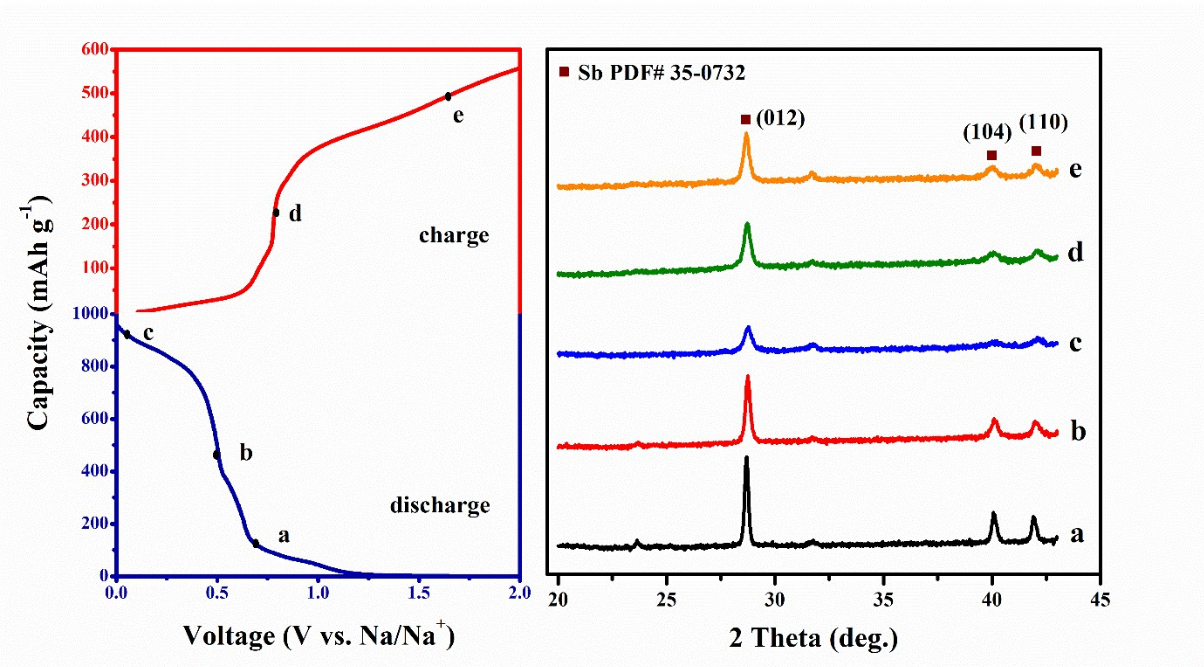

Figure S26. *Ex situ* XRD patterns of the Sb-Nb_2O_5 nanomeshes at different discharge-charge voltages.

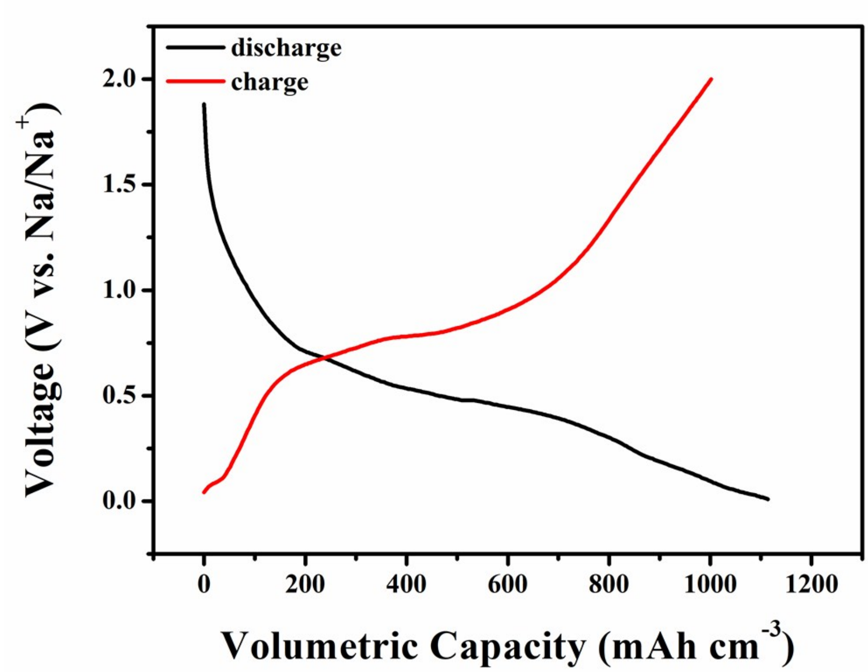

Figure S27. Selected charge-discharge profiles of the synergic Sb-Nb_2O_5 nanomeshes at a current density of 0.05 mA cm^{-2}, delivering a reversible volumetric capacity of 1001 mAh cm^{-3}.

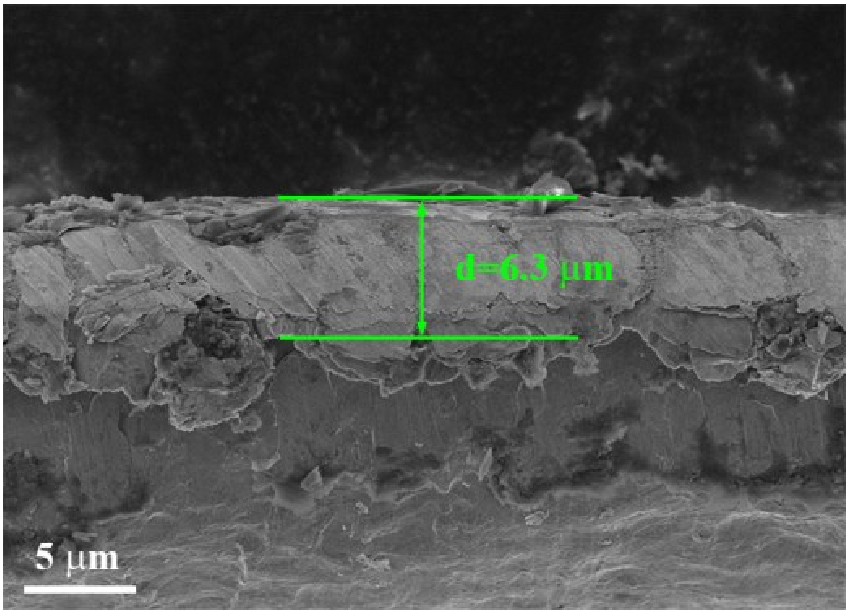

Figure S28. Cross-section SEM image of electrode with mass loading of 1.45 mg.

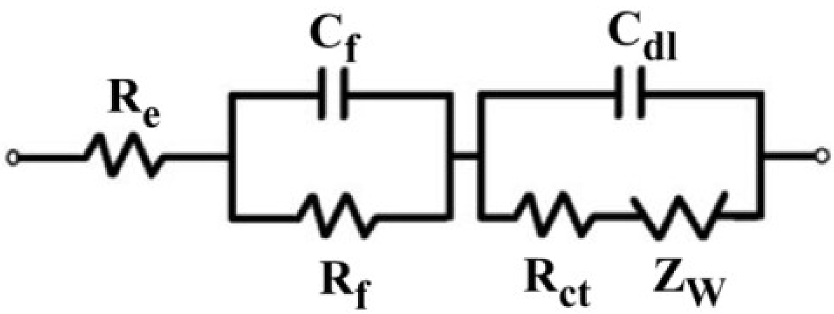

Figure S29. Modified Randles equivalent circuit for the electrode/electrolyte interface of the synergic Sb-Nb_2O_5 nanomeshes, $Nb_2O_5{\cdot}nH_2O$ nanosheets, $SbNbO_4$ nanosheets and Sb particles. R_e, R_f and R_{ct} stand for the electrolyte resistance, surface resistance and charge-transfer resistance, respectively. C_f and C_{dl} are the surface capacitance and double-layer capacitance, respectively. Z_w represents the Warburg impedance related to the diffusion of sodium ions into the bulk electrodes.

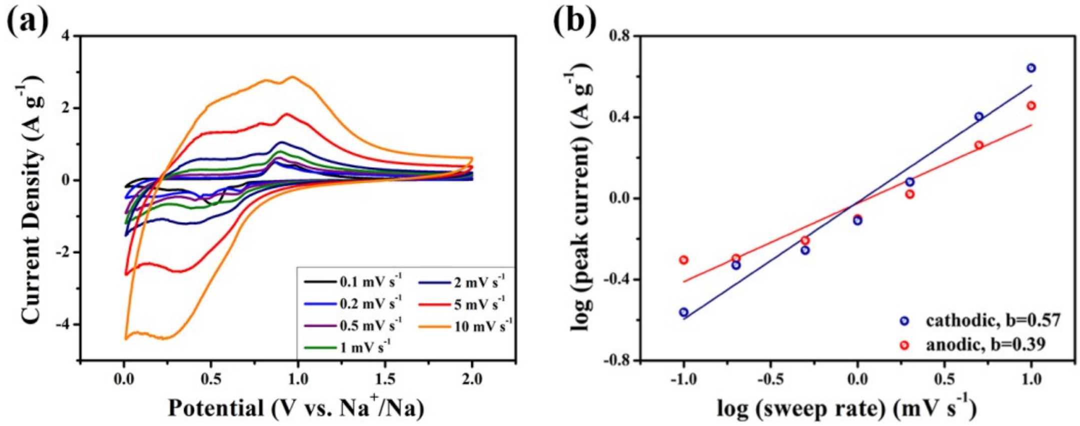

Figure S30. (a) Cyclic voltammograms of Sb particles at the sweep rates of 0.1 to 10 mV s^{-1}. (b) Plots of log (i) versus log (v) of both anodic and cathodic peaks (circles) and b-value determination (lines) according to the relationship: i=av^{b}.

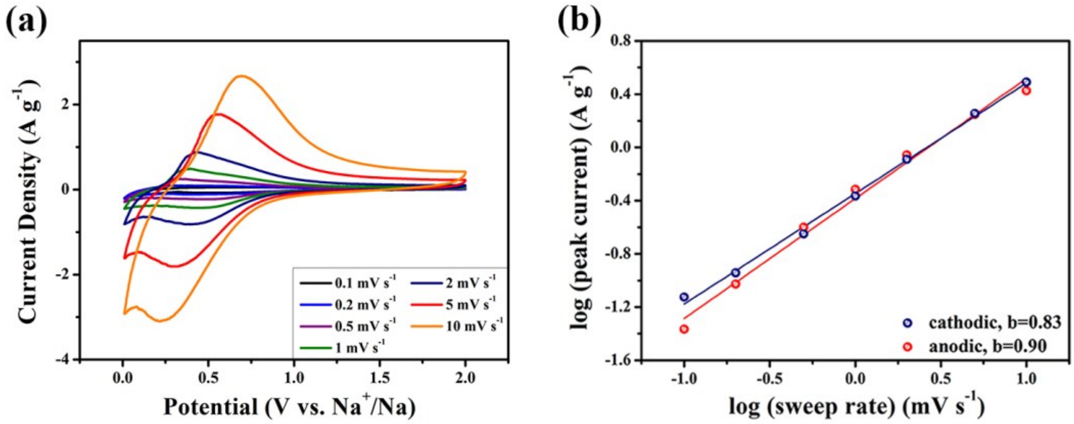

Figure S31. (a) Cyclic voltammograms of $Nb_2O_5{\cdot}nH_2O$ nanosheets at the sweep rates of 0.1 to 10 mV s^{-1}. (b) Plots of log (i) versus log (v) of both anodic and cathodic peaks (circles) and b-value determination (lines) according to the relationship: i=av^b.

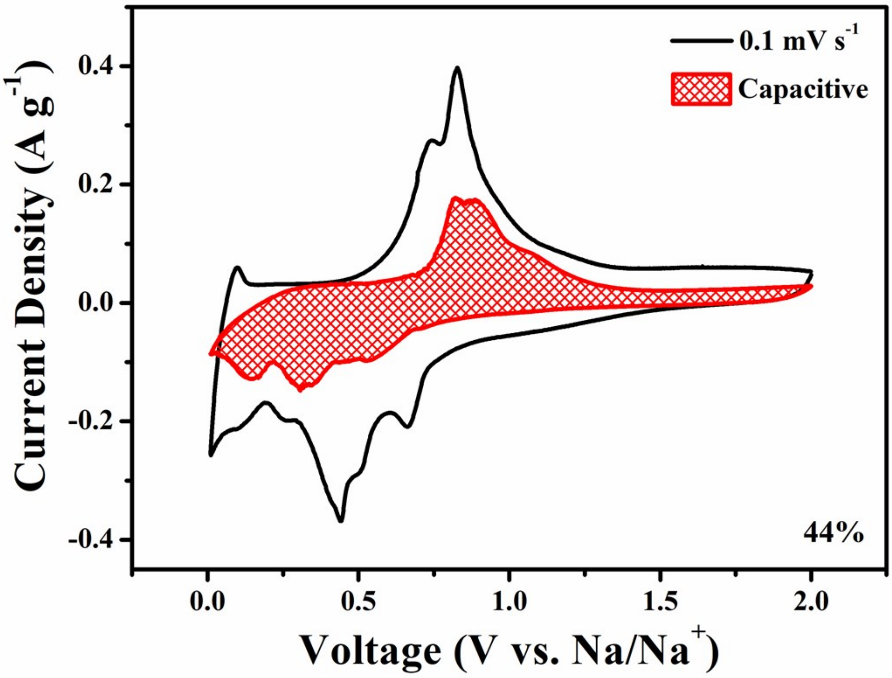

Figure S32. CV profiles with capacitive current separation of Sb-Nb_2O_5 nanomeshes at 0.1 mV s^{-1}, delivering 44% capacitive contribution of the total capacity.

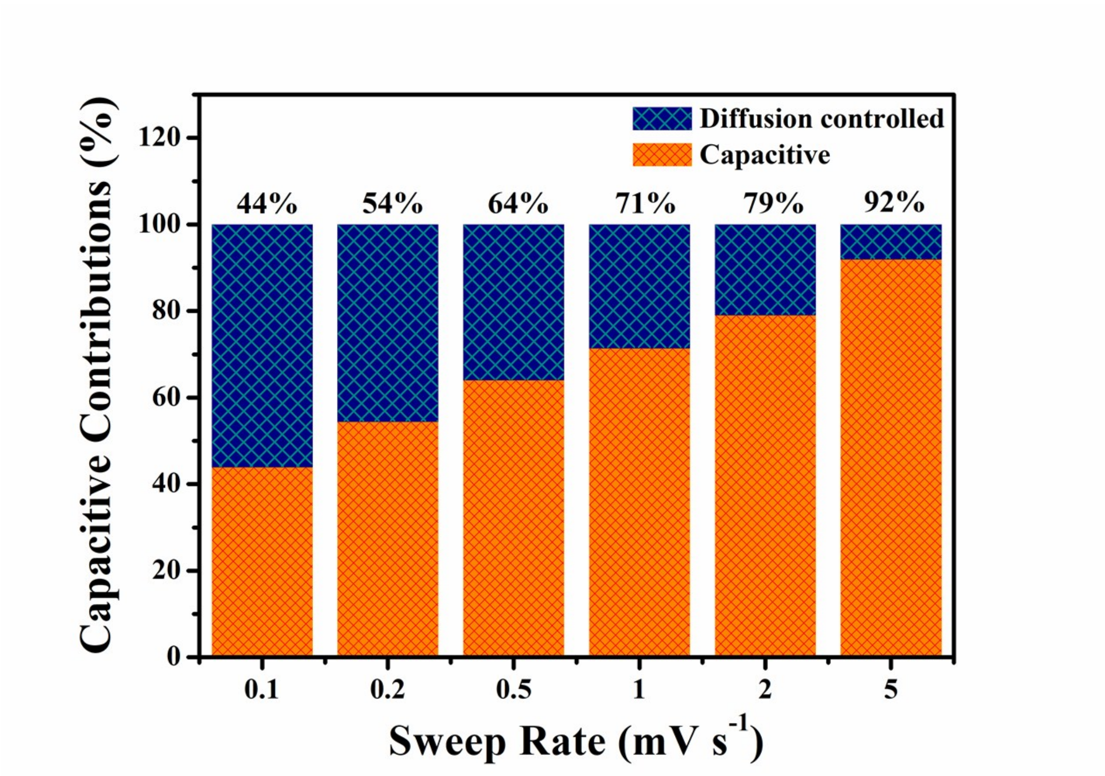

Figure S33. Capacitive and diffusion controlled capacity contributions of Sb-Nb_2O_5 nanomeshes at various sweep rates ranging from 0.1 to 5 mV s^{-1}.

Table S1. Progress on systhesis of Sb-based and Nb-based materials and their electrochemical performances for sodium storage

Materials	Synthesis method	Reversible capacity [a)]	Rate capability [b)]	Ref.
Sb-Nb_2O_5 nanomeshes	Hydrothermal and heat treatment	558/0.1	190/10	This work
Sb/SiOC	Sonication and pyrolysis	510/0.05 C	453/20 C	40
Sb@TiO_{2-x} nanotubes	Solvothermal, hydrolysis and heat treatment	601/0.066	312/13.2	22
Few-layer antimonene	Liquid-phase exfoliation	642/0.066	429/3.3	42
Sb nanosheets	Liquid-phase exfoliation	463/0.062	82/2.5	12
Sb/C fibers	Electrospinning and heat treatment	422/0.1	88/6	11
$TiNb_2O_7$/graphene	Freeze dying and heat treatment	311/0.025	146/0.5	41
Nb_2O_5@C/rGO	Sol-gel and heat treatment	285/0.025	109/3	19
G-Nb_2O_5 nanosheets	Nanocasting and heat treatment	230/0.05	100/2	20
a-H-Nb_2O_5 film	Anodization and heat treatment	185/0.1	84/2	18

a) The reversible capacity is summarized as capacity/corresponding current density. b) The rate capability is summarized as capacity/corresponding current density. The unit of capacity is mAh g^{-1}, and the unit of current density is A g^{-1}.

Table S2. Kinetic parameters of the synergic Sb-Nb_2O_5 nanomeshes, $Nb_2O_5 \cdot nH_2O$ nanosheets, $SbNbO_4$ nanosheets and Sb particles.

Sample	R_e Ω	R_{ct} Ω	σ_w Ω $s^{-1/2}$	D $cm^2\ s^{-1}$
synergic Sb-Nb_2O_5 nanomeshes	10.8	49.7	490.4	1.15×10^{-13}
$Nb_2O_5 \cdot nH_2O$ nanosheets	12.1	151.7	1176.2	2.00×10^{-14}
$SbNbO_4$ nanosheets	13.5	128.6	584.2	8.13×10^{-14}
Sb particles	13.1	129.3	746.8	4.97×10^{-14}